

Secondary-Electron Yield on Copper-Beryllium for H^+ , H_2^+ , H_3^+ , H^0 , H_2^0 , and H_3^0 *

E. S. CHAMBERS

Lawrence Radiation Laboratory, University of California, Livermore, California

(Received 26 September 1963)

Experimental secondary-electron yields for H^+ , H_2^+ , and H_3^+ incident on copper-beryllium at 60° increase continuously from about 3 at 2 keV to 5.9 at 55 keV for H^+ ; to 8.5 at 55 keV for H_2^+ ; and to 10.8 at 55 keV for H_3^+ . At an angle of incidence 0° – 72° corresponding values are about 1.7 times larger. Thus the yield increases approximately as $\sec\theta$. The ratio of yield δ_0 for neutral particles (obtained by charge transfer) to yield δ_1 for ions was determined by a calorimetric measurement of the incident beam power. Neutrals yield more electrons than ions, and the ratio is only slightly dependent on energy. At 25 keV, the ratio δ_0/δ_1 is 1.14 for H^+ , 1.26 for H_2^+ , and 1.41 for H_3^+ . The secondary-electron and positive-ion energy spectra were measured for both neutrals and ions. The two types of particles gave the same spectra. The atomic stopping cross section for protons on copper was extrapolated down to 2 keV.

INTRODUCTION

SECONDARY-ELECTRON emission is an interesting, though complex, phenomenon resulting from the interaction of bombarding particles, such as electrons or ions, with a solid. An experimental study is useful in learning the details of such interactions as well as in developing sensitive, energy-dependent particle detectors. A number of reviews cover secondary-electron emission for both electrons and ions^{1,2} and electrons^{3–6} alone.

The secondary-electron yields for 9–60-keV H^+ , H_2^+ , H_3^+ , and H^0 on copper-beryllium at a 60° angle of incidence were measured by Schwirzke.⁷ The ratio of secondary-electron yields for H atoms to that for H^+ ions was found by Stier *et al.*⁸ to be 1.11 at 20 keV and 1.16 at 60 keV, using nickel at 0° . The yield ratio for H^0 , H^+ on aluminum, was calculated by Ghosh and Khare⁹ to be about 1.0 between 20 and 60 keV.

This paper describes yield data between about 2 and 55 keV for H^+ , H_2^+ , and H_3^+ on copper-beryllium at 60° and 72° . The ratio of yield for a neutral to that for a corresponding ion was obtained by a calorimetric comparison for H, H_2 , and H_3 . The secondary-electron energy spectra for H_2^0 and H_2^+ are compared at 10 and 15 keV.

When a beam of sufficiently energetic particles impinges on a metal, electrons within the metal acquire energy by Coulombic interaction. These energetic elec-

trons interact with the electrons about them, changing momentum and losing energy. If, however, electrons reach the surface with an energy greater than the work function, they may become secondary electrons. An ion in the kilo-electron-volt range loses only a small fraction of its energy at each collision and is not appreciably deviated. Its penetration depth will be long compared with the path length of an accelerated electron, which can lose a large fraction or even all of its energy in a single impact. For this reason the rate of ion energy loss dE/dx will be approximately constant over the range where the secondaries originate. Thus, the effect of bombarding ions is easier to interpret than the effect of bombarding electrons of similar velocity.

EXPERIMENT

The apparatus used for this work is shown in Fig. 1. Details of the ion source, analyzing magnet, beam collimator, drift space (in which charge transfer took place), deflector electrodes, and detector collimator have been described.¹⁰ The target consisted of Berylco 25 from the

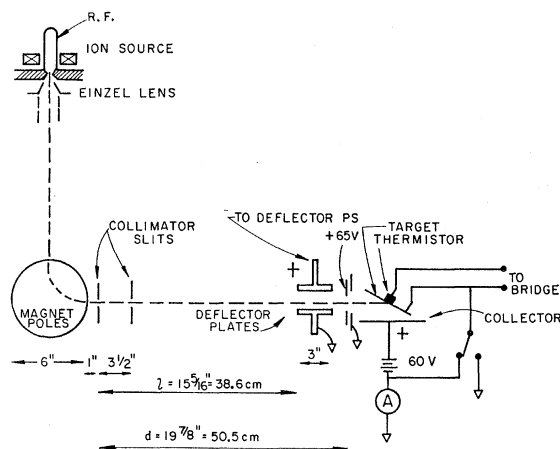


Fig. 1. Apparatus for secondary-electron yield determination.

¹⁰ E. S. Chambers, Lawrence Radiation Laboratory (Livermore) Rept. No. UCRL-6987 (unpublished).

* Work done under the auspices of the U. S. Atomic Energy Commission.

¹ H. S. W. Massey and E. H. S. Burhop, *Electronic and Ionic Impact Phenomena* (Clarendon Press, Oxford, England, 1952).

² A. von Engel, *Ionized Gases* (Clarendon Press, Oxford, England, 1955).

³ H. Bruining, *Physics and Applications of Secondary Electron Emission* (McGraw-Hill Book Company, Inc., New York, 1954).

⁴ A. J. Dekker, *Solid State Phys.* **6**, 251 (1958).

⁵ K. G. McKay, *Advan. Electron.* **1**, 65 (1948).

⁶ J. S. Allen, Preliminary Report No. 10, Nuclear Science Series, National Research Council, 1950 (unpublished).

⁷ F. Schwirzke, *Z. Physik* **157**, 510 (1960).

⁸ P. M. Stier, C. F. Barnett, and G. E. Evans, *Phys. Rev.* **96**, 973 (1954).

⁹ S. N. Ghosh and S. P. Khare, *Phys. Rev.* **129**, 1638 (1963).

Beryllium Corporation, a copper-beryllium alloy, temper $\frac{1}{4}H$. This predominantly copper alloy contains 1.83–2.05% Be, 0.20–0.30% Co, 15% max Fe, 0.15% max Si, and smaller amounts of Al, Sn, Pb, Ni, Cr, Zn, and Ag. It was used as received after polishing with No. 600 silicon carbide paper and cleaning with acetone. One target was heat treated and electropolished as prescribed by Michijima.¹¹ However, no significant increase in the yield was obtained. The ion beam changed the bright copper colored targets to a yellow which shaded to a blue in the center of highest current density. The treated target was not colored, although the exposure was probably smaller. No doubt, both target surfaces were influenced by vacuum system contamination.

The target could be switched to either a Keithley model 415 micromicroammeter when the net current was read, or to ground when the secondary-electron current was read. For the calorimetric comparison of neutrals and ions, the target was $0.005 \times 0.53 \times 0.37$ in. All targets were flat and adjusted to the desired angle of incidence to within about a degree. A D-052 thermistor with a resistance of about 2000Ω and a temperature coefficient of $41\Omega/^\circ\text{C}$ was used to measure the target temperature. It was connected to a conventional bridge using a Fluke 801 HR differential dc voltmeter as a null detector. The time constant of the target system was 0.5 min so that 3 or 4 min of steady operation was required for a reading. Further details of the calorimetry are discussed in another paper.¹²

Data for obtaining the secondary-electron yields were recorded at the same time charge-transfer cross sections were obtained. The yield δ was obtained by dividing the secondary-electron current from ions, i_{se} , by the ion current i_i . However, the total secondary-electron current is $i_{st} = i_{se} + i_{sn}$, where i_{sn} is the secondary current caused by the neutral atoms that resulted from charge transfer in the drift space. The i_{sn} component was obtained directly by deflecting the ions before reaching the detector. A geometrical correction factor d/l (see Fig. 1) adjusts this component to account for loss of ions by charge transfer between the front edge of the deflector and the detector slit. Thus, the yield for ions only is $\delta = (i_{st} - i_{sn}d/l)/i_i$.

In the calorimetric comparison of the yields from neutrals and ions, a hydrogen pressure of about 2×10^{-4} mm Hg in the drift region converted roughly 20% of the ions to neutrals. The remainder of the ions were deflected into the bottom electrode. After several minutes of steady operation the thermistor approached a constant higher temperature and the bridge unbalance was measured. At the same time the secondary-electron current was read. Then the ion current was reduced and adjusted to give about the same secondary-electron current with no deflection voltage. The resulting thermistor temperature was then approximately that in

the neutral case and the yield ratio is $\delta_0/\delta_1 = i_{sn}\Delta T_i/i_{se}\Delta T_n$, where $\Delta T_i/\Delta T_n \approx 1$ is the ratio of the temperature rises. In this way an absolute calibration was not required. The calorimeter was used essentially as a null instrument.

A retarding potential analysis of the secondary-electron energy distribution was made by introducing a variable potential difference between the target and the collector. The secondary-electron current was measured as a function of this potential difference.

In all these experiments the target surface was exposed to an environment of about 10^{-4} mm Hg H_2 and the vapor pressure of Dow Corning 704 fluid, rubber, and Viton gaskets. In spite of this, there was only a minor decrease in yield over a period of many weeks which includes several periods at "air." Part of this stability may be attributed to the depth of penetration of the heavy ions (compared to electrons) which would minimize the effect of the surface film.

In the yield ratio experiments the precision for the H^0 , H^+ points is about $\pm 2\%$. However, in the H_2^+ and H_3^+ experiments the precision is about $\pm 6\%$. At the lower energies this decrease in precision is expected since the power incident on the target becomes small and the temperature rise uncertain. Also, with H_3^+ the ion current throughout was small. Over most of the range, however, the H_2^+ current was about $5i_{\text{H}^+}$ and $20i_{\text{H}_3^+}$, and the target temperature should be reproducible to about 1%.

RESULTS

The secondary-electron yields as a function of the ion energy for hydrogen ions, H^+ , H_2^+ , H_3^+ on Cu-Be for a 60° angle of incidence are shown in Fig. 2. The curves rise continuously to a yield, at 55 keV, of 5.9 for H^+ , 8.5 for H_2^+ , and 10.8 for H_3^+ . The high-energy slopes of the curves increase in the order, H^+ , H_2^+ , and H_3^+ .

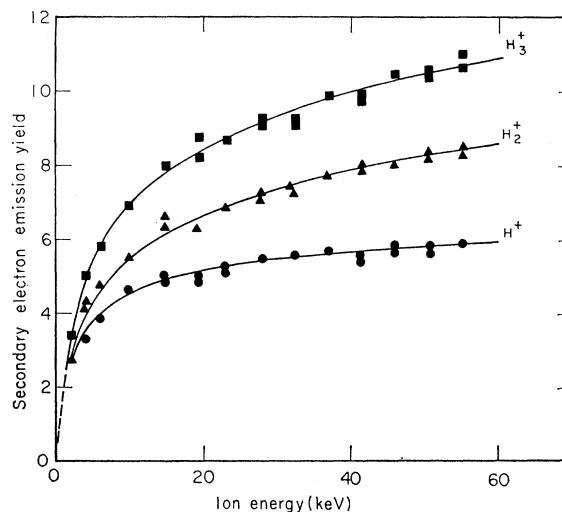


FIG. 2. Secondary-electron yield of hydrogen ions on copper-beryllium (Berylco 25) vs ion energy for 60° angle of incidence.

¹¹ M. Michijima, J. Appl. Phys. Japan **1**, 110 (1962).

¹² E. S. Chambers, Rev. Sci. Instr. **36**, 95 (1964).

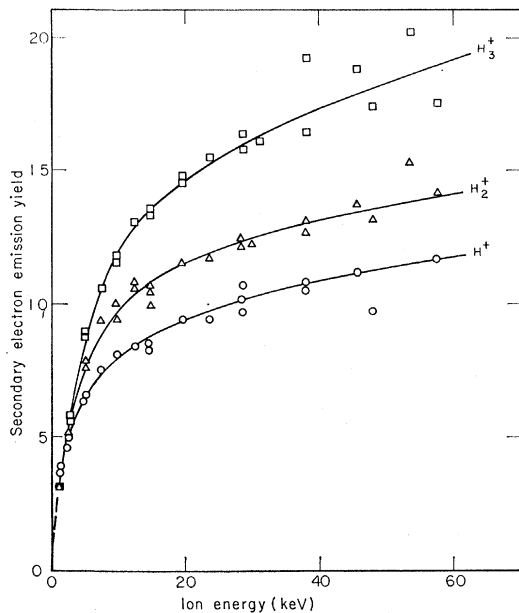


FIG. 3. Secondary-electron emission yield vs ion energy for hydrogen ions on copper-beryllium at 72°.

Most of Schwirzke's⁷ data are about 10% higher. His H_2^+ value at 10 keV is 23% higher, while at 60 keV H^+ and H_2^+ are 5% and H_3^+ , 2% higher. The agreement is reasonable considering that his target may have had a slightly different composition and surface treatment.

The yield for H^+ , between 2 and 20 keV, was essentially identical at the two pressures, 7.6×10^{-5} and 2.0×10^{-4} mm Hg. A number of runs with 10- and 15-keV H_2^+ showed the same yield within a few percent when the pressure was varied between 2×10^{-6} and 2×10^{-4} mm Hg.

Similar secondary-electron yield versus ion energy data are shown in Fig. 3 for an angle of incidence of 72°.

The ratio of the secondary-electron yield produced by a neutral particle to the yield from the corresponding

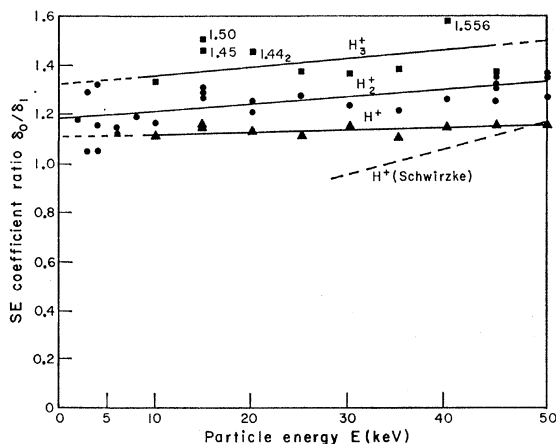


FIG. 4. Ratio of secondary-electron yield from neutrals and ions as a function of energy (on Cu-Be at 60°).

ion, δ_0/δ_1 , is shown in Fig. 4 for an angle of incidence of 60°. The ratios are fairly constant with energy, and may be approximated, above 8 keV, by the equations

$$H: \delta_0/\delta_1 = 1.11 + 0.001E,$$

$$H_2: \delta_0/\delta_1 = 1.18 + 0.003E,$$

$$H_3: \delta_0/\delta_1 = 1.32 + 0.003E,$$

where E is the ion energy in keV. The points of Fig. 4 suggest that the curves may not be as linear as drawn. The data of Stier *et al.*⁸ for H^0 , H^+ on Ni at 0° agree very closely, suggesting that Ni is similar to Cu-Be in this respect. Schwirzke's δ_0/δ_1 curve stays below 1 at lower energies.

Retarding-potential analysis data of total collector current versus collector voltage for 10-keV H_2^0 is shown in Fig. 5. The corresponding curve for 10-keV H_2^+ was

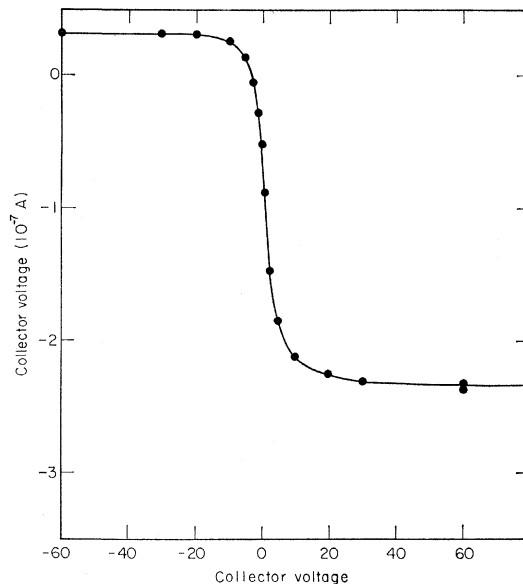


FIG. 5. Retarding potential analysis of secondary particles from 10-keV H_2^0 on Cu-Be at 60°.

similar. Both positive and negative particles are emitted from the target. When the collector voltage is zero with respect to the target, both components are collected and the algebraic sum will be measured. The positive component was obtained from the current at -90 V; the negative component from the current at +60 V. The sum of these components indicates that the actual electrode potential zero would be at +6 V on the curve. This difference from the applied potential can be attributed to the contact potential difference between the Cu-Be target and the Cu collector and surface charge effects.

Employing the 6-V displacement, the secondary-electron energy distribution is obtained by graphical differentiation and is shown in Fig. 6 for the 10-keV H_2^0 , which is almost identical to the 10-keV H_2^+ curve. The

corresponding energy distribution of the positive-ion component is shown in Fig. 7. Curves for both H_2^0 and H_2^+ are shown; the difference could be within experimental error.

The repulsion analysis was repeated for 15-keV H_2^+ , and H_2^0 , using an x - y plotter to detect any fine structure in the curve. None was found. The curves for both neutrals and ions were similar and had a form similar to those described above. With ions no difference was seen at the two pressures 5.5×10^{-6} and 1.1×10^{-4} mm Hg.

DISCUSSION

The proportionality between the secondary-electron yield δ and the space rate of energy loss dE/dx has been demonstrated by Kanter,¹³ and Schultz and Pomerantz¹⁴

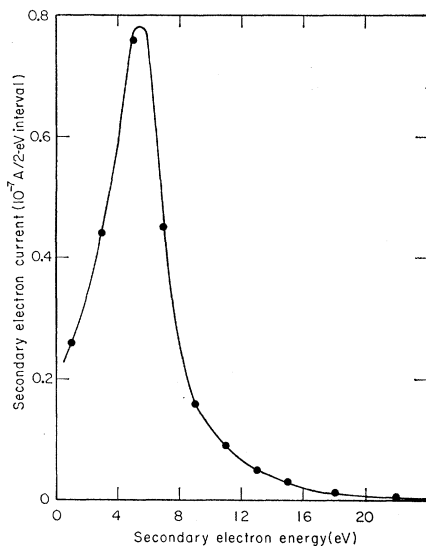


FIG. 6. Secondary-electron energy distribution for 10-keV H_2^0 on Cu-Be at 60° .

for electrons (>1 keV) on C, Al, or Ni. Assuming that the same holds for protons, a knowledge of the secondary-electron yield can be used to extend the atomic stopping power data of Whaling¹⁵ for protons on copper. This has been done in the upper extrapolation of Fig. 8, normalizing to his lowest (50 keV) point. The points from both the 60° and 72° data agree within 10%. A preliminary extrapolation, based on similarity to the oxygen curve, is shown for comparison.

Based on the equation¹⁴ $\delta = (\Delta X/\epsilon)(dE/dx)\text{sec}\theta$, where ΔX is the thickness of the region where escaping secondary electrons are produced, and ϵ the average energy to produce one electron, the average energy dissipation density to produce one secondary electron is $\epsilon/\Delta X$

¹³ H. Kanter, Phys. Rev. **121**, 677 (1961).

¹⁴ A. A. Schultz and M. A. Pomerantz, Phys. Rev. **130**, 2135 (1963).

¹⁵ W. Whaling, National Academy of Sciences, National Research Council Publication 752, 1960, p. 1.

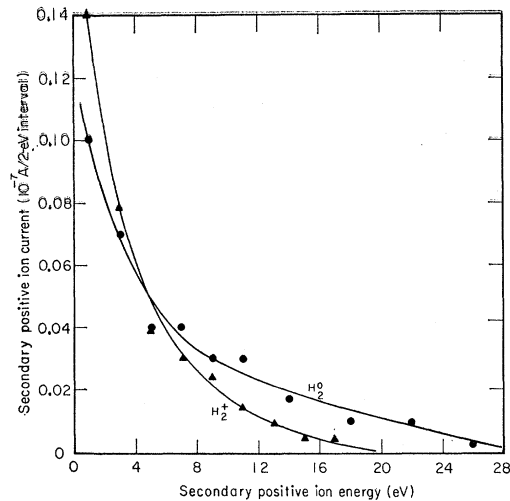


FIG. 7. Secondary positive ion energy distribution for 10-keV H_2^0 or H_2^+ on Cu-Be at 60° .

$= (dE/dx)(1/\delta)\text{sec}\theta$. The present data give for protons on copper-beryllium $\epsilon/\Delta X = 66$ eV-cm²/μg. This is somewhat lower than reported values¹⁴ of 90 and 100 eV-cm²/μg for electrons on Al and N, respectively.

Using the upper curve of Fig. 8, the stopping-power cross section for 10-keV protons in copper is 15.7×10^{-16} eV-cm². Thus, even after a path of 744 Å there will still be 37% of the original energy in the ions. Bruining and de Boer¹⁶ estimated the mean depth of production of secondary electrons was 30 Å in Li for 500-eV electrons. Becker¹⁷ calculated a mean depth in nickel of about 30 Å. This indicates that for a 10-keV proton in copper, only electrons, produced along the first part of the path, will be able to escape from the surface. Thus dE/dx will be substantially constant. The secondary-electron yields for the three different ions may be compared at the same ion velocity. In Fig. 9 this is done by plotting yield against the equivalent energy, which is the energy of an electron traveling at the same velocity as the ion.

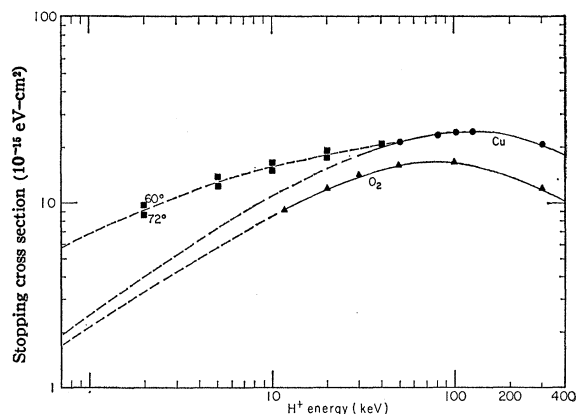


FIG. 8. Atomic stopping cross sections for protons.

¹⁶ H. Bruining and J. H. de Boer, Physica **5**, 17 (1938).

¹⁷ A. Becker, Ann. Physik (Leipzig), **2**, 249 (1929).

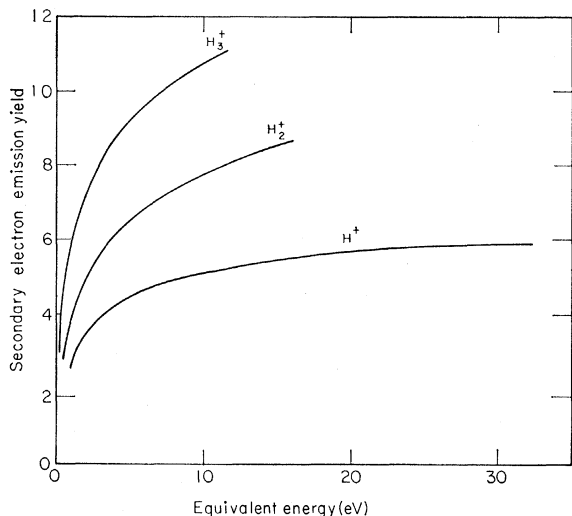


FIG. 9. Secondary-electron yield of hydrogen ions on Cu-Be at 60° vs velocity as measured by electron energy of same velocity.

The results indicate that the separate nucleons of the molecular ions act almost independently of each other. The efficiency of each nucleon as compared with a single one is 0.74 in H_2^+ and 0.69 in H_3^+ .

It is possible that the secondary-electron yield depends on the vibrational state of a molecular bombarding particle, such a state being determined by ion source conditions. The data of McClure¹⁸ show that dissociation on gas may take place. In these experiments roughly 5% of the ions would be affected.

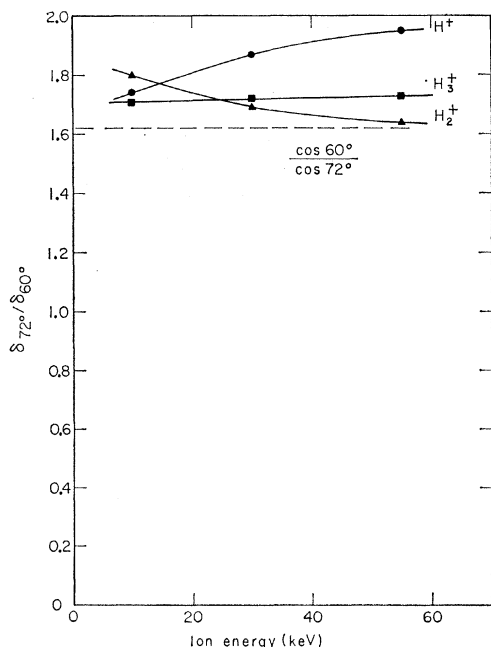


FIG. 10. Ratio of the secondary-electron yields at 72° and 60° as a function of energy.

¹⁸ G. W. McClure, Phys. Rev. **130**, 1852 (1963).

From the location of the peak of the stopping cross-section curve it is predicted that for H^+ the maximum secondary-electron yield will occur at a proton energy of 125 keV. For H_2^+ this energy would be 250 keV, and for H_3^+ , 375 keV.

The dependence on angle of incidence may be obtained by comparing the data of Figs. 2 and 3. Figure 10 shows the ratio δ_{72}/δ_{60} as a function of energy for the three ions. The expected ratio is $\cos 60^\circ/\cos 72^\circ$ if the simple relation $\delta_\theta = \delta_0 \sec \theta$ is obeyed. This equation applies if the ion range is much longer than the secondary-electron range in the metal and if these electrons are produced isotropically. In such a case, the energy loss per unit length along the first part of the ion path, where "fresh" secondary electrons are produced, will be constant. For any given distance d from the surface the ion path length $l = d/\cos \theta$ and, hence, the yield will be increased by the factor $\sec \theta$. However, a relatively free conduction electron would tend to be accelerated at 90° to the ion path. Although subsequent scattering would make the velocity more isotropic, this effect would increase the yield still higher at large angles of incidence.

The ratio of neutral yield to ion yield, δ_0/δ_1 , (Fig. 4) shows that a neutral produces more secondary electrons than an ion does and the fractional increase is only slightly dependent on energy. Consider the neutral H^0 , and assume that the H^0 electron moving along at the same velocity with the proton can independently produce secondary electrons. For a 6.06-keV H^+ the energy of an electron moving at the same velocity is 3.3 eV. As it drops down the potential barrier into the metal it will gain the work function energy ϕ . In a collision with another electron, the maximum energy transfer is $E_e = E_0 + \phi$. In this case for Cu, $E_e \approx 7.7$ eV, and after some loss required to deflect the electron toward the surface, it is possible that it can still overcome the work function and become a secondary electron.

For bombarding particle of mass m_1 and target of mass m_2 , the maximum energy transferred¹⁹ is given by $T_m = [4m_1m_2/(m_1+m_2)]E_1$. For H^+ striking an electron $T_m = 2.18 \times 10^{-3}E$ and, hence, for the 6.06-keV H^+ , $T_m = 13.2$ eV. Thus $E_e/T_m = 0.58$ and at higher energies where the work function is less important this approaches $3.3/13.2 = 0.25$. If the work function is neglected, the ratio will be independent of energy and is $1 + 0.25/1 = 1.25$. Actually the data show, for H^0 and H^+ , that $\delta_0/\delta_1 \approx 1.14$. The explanation for this lower-than-expected value may be that the electron is held so closely to the H^+ that each can not affect as many electrons in the metal as they would if acting independently.

For H_2^+ at the same velocity as the H^+ , $E(H_2^+) = 2E(H^+)$. Also, $T_m(H_2^+) = \frac{1}{2}T_m(H^+)$ and, hence, in the

¹⁹ F. Seitz and J. S. Koehler, Solid State Phys. **2**, 305 (1956).

example where $E(e^-) = 3.3$ eV, energy transferred from the ion will be $T_m = 13.2$ eV, and the energy ratio will be the same as before. However, H_2^+ holds an outer electron somewhat less firmly than does H^+ , and the

two act more independently, hence, affecting more electrons. A similar argument holds for H_3^+ . The dissociation of the neutrals¹⁸ will also contribute to the higher δ_0/δ_1 ratios.

Galvanomagnetic Effects in Heavily Doped *p*-Type Germanium*

G. SADASIV

Department of Physics, Purdue University, Lafayette, Indiana

(Received 11 July 1963; revised manuscript received 9 September 1963)

The Hall effect and magnetoresistance in heavily doped *p*-type germanium have been measured. The samples had gallium impurity concentrations between 10^{18} and 10^{19} cm⁻³. The measurements were made at 77, 20.4, 4.2, and 1.4°K, with magnetic fields ranging up to 30 kG. The results are compared with the predictions of simple transport theory applied to carriers in the unperturbed valence band of germanium. The data at 77°K can be adequately described on the basis of this model. At very low temperatures, however, the data are in disagreement with the predictions of the model. The magnetoresistance effects, in particular, are anomalous; the transverse component shows a linear dependence on magnetic field, and a longitudinal magnetoresistance is observed.

1. INTRODUCTION

THIS paper describes an investigation of galvanomagnetic effects in heavily doped *p*-type germanium. The samples had gallium impurity concentrations between 10^{18} and 10^{19} cm⁻³. The measurements were made at 77, 20.4, 4.2, and 1.4°K, with magnetic fields ranging up to 30 kG.

To a rough approximation the ground state of a hole in a localized level around a gallium impurity is described by an effective Bohr radius of 70 Å.¹ When there are more than 10^{18} gallium atoms per cm³, the neighboring impurities are so close together that the concept of states localized around an impurity loses its meaning.

The band structure in such disordered materials has been the subject of several theoretical investigations,² but as yet there is no agreement about the nature and the density of the carrier states. Many of the experimental studies of such materials, however, yield results which are consistent with the following model. The carriers are assumed to occupy states in the unperturbed band; as the temperature is lowered there is no freeze out so that the number of carriers remains constant, the only effect is to change the degree of statistical degeneracy of the carriers. For example, the magnetic susceptibility³ and infrared reflectivity⁴ of

n-type germanium have been measured. The density of states effective mass deduced from these experimental results agrees with the value found by cyclotron resonance experiments on pure samples. Keesom and Seidel⁵ measured the specific heat of *n*- and *p*-type samples in the temperature range between 0.5 and 4.2°K. Their experiments determine essentially the density of states at the Fermi level, and the results are in agreement with the values calculated on the basis of a degenerate Fermi gas in the unperturbed band.

The purpose of the present investigation was to measure the Hall effect and magnetoresistance in *p*-type germanium, and compare the results with the predictions of simple transport theory applied to such a model. The results at 77°K are in reasonable agreement with the theory. However at liquid-helium temperatures the galvanomagnetic effects show an anomalous behavior. The most striking features are a linear dependence of the transverse magnetoresistance on the magnetic field and the presence of a longitudinal magnetoresistance.

2. TRANSPORT THEORY FOR A TWO-BAND MODEL

The structure of the valence band in pure germanium is known from cyclotron resonance experiments.^{6,7} The surfaces of constant energy are two sets of warped spheres and degenerate at $k=0$. These give rise to two kinds of holes, the heavy and the light ones; the ratio of the number of heavy holes to the number of light

* Work supported by U. S. Army Research Office.

¹ S. Golin, *Bull. Am. Phys. Soc.* **8**, 224 (1963).

² *Proceedings of the International Conference on the Physics of Semiconductors, Exeter, 1962* (The Institute of Physics and the Physical Society, London); see papers by V. L. Bonch-Bruевич, p. 216; E. M. Conwell and B. W. Levinger, p. 227; P. A. Wolff, p. 220.

³ R. Bowers, *Phys. Rev.* **108**, 683 (1957).

⁴ W. G. Spitzer, F. A. Trumbore, and R. A. Logan, *J. Appl. Phys.* **32**, 1822 (1961).

⁵ P. H. Keesom and G. Seidel, *Phys. Rev.* **113**, 33 (1959).

⁶ G. Dresselhaus, A. F. Kip, and C. Kittel, *Phys. Rev.* **98**, 368 (1955).

⁷ D. M. S. Bagguley, R. A. Stradling, and J. S. Whiting, *Proc. Roy. Soc. (London)* **A262**, 340 (1961).